Supporting Information

Berry et al. 10.1073/pnas.1112057109

SI Materials and Methods

The translational diffusion coefficient of α_3Y was determined by pulsed field gradient experiments as described in ref. 1. NMR spectra were collected at 25 °C on a 500 MHz Bruker Advance III spectrometer equipped with a cold probe. 500 μM α_3Y was dissolved in a 20 mM deuterated sodium acetate, 20 mM potassium phosphate, 20 mM sodium borate, 140 mM KCl, 5% D_2O, pH 6.6 buffer. Differential pulse voltammetry (DPV) (2, 3) and square-wave voltammetry (SWV) (2, 4, 5) were performed using an Autolab PGSTAT12 potentiostat equipped with a temperature-controlled, Faraday-cage protected three-electrode micro-cell (Princeton Applied Research). The Ag/AgCl reference electrode and the platinum wire counter electrode (Advanced Measurements Inc.) were stored dry and prepared by filling the former with a 3 M KCl/saturated AgCl solution and the latter with sample buffer. DPV measurements were carried out using a 3 mm diameter glassy carbon working electrode (Advanced Measurements Inc.). The surface of the glassy carbon electrode was carefully polished between each measurement using a 0.05 μm alumina/water slurry on a glass-plate mounted microcloth pad (Bioanalytical systems Inc.). The electrode was manually polished for 60 s, rinsed with water, sonicated in ethanol for 60 s, in milli-Q water for another 60 s, and finally rinsed with an excess of milli-Q water directed against the surface of the electrode. Some DPV and all SWV measurements were carried out using a 3 mm diameter pyrolytic graphite edge electrode (Bio-Logic, USA). The electrode surface was activated between measurement by manually polishing its surface for 60 s in a 1.0 μm diamond/water slurry on a diamond polishing pad (Bio-Logic, USA) followed by 60 s in a 0.05 μm alumina/water slurry on a microcloth pad (Bioanalytical systems Inc.). The electrode was rinsed with an excess of methanol followed by milli-Q water directed against the surface of the electrode. Measurements were performed immediately following the polishing procedures. The electrochemical cell was also fitted with a pH electrode (Microelectrodes Inc.) connected to a SevenMulti pH meter (Mettler Toledo). The pH was routinely monitored between voltammetry runs. The pH electrode was disconnected from the pH meter during the active voltammetry measurements to avoid the risk of introducing electric noise. The response and reproducibility of the fully assembled electrochemical cell were checked at the beginning of each experimental day by using standard samples and settings. IR compensation was performed by using the Autolab positive feed-back function. Potentials are given vs. the NHE. All samples were prepared from ultra-pure chemicals and the measurements performed under an argon atmosphere. Protein concentration, KCl concentration, and pH series were obtained by equal-volume titrations. Data processing and analyses were performed using the Autolab GPES software, KaleidaGraph (Synergy Software), and PeakFit (Systat Software Inc.). DPV half-wave potentials ($E_{1/2}$) were derived from the observed DPV peak potentials (E_{peak}) using the Parry-Osteryoung relationship $E_{1/2} = E_{peak} + \Delta E/2$ where ΔE is the modulation amplitude (3). The α_3Y Pourbaix diagram (Fig. 1*F*, main text) was fitted to Eq. **1** by nonlinear regression. The $E_{1/2}$ vs. pH profile was first simulated using Excel in order to find starting values. Data fitting and evaluations of the data fits were conducted using the GraphPad Prism program (GraphPad Software).

Summary of Voltammetry Raw Data, Data Processing, and Error Analyses

Data series were obtained by typically collecting three to four voltammograms per data point. Fig. S2*A* displays a representative α_3Y DPV raw-data triplicate. Fig. S5*A*–*F* show typical α_3Y SWV raw-data triplicates representing the net current, the forward (oxidation) current, and the reverse (reduction) current. Correction of background currents was performed by fitting a cubic baseline to the raw voltammograms. An example of a raw DP voltammogram with a fitted baseline is shown in Fig. S2*B*. Fig. S4 displays examples of raw net, forward, and reverse SW voltammograms with fitted baselines and the resulting background-corrected data. DPV half-wave potentials ($E_{1/2}$) were obtained by first-derivative analysis (Fig. S2*C*–*F*) or by fitting a calculated line to the raw voltammogram (Fig. S2*G* and *H*). The average error in $E_{1/2}$ representing data replicates is ±3 mV. There was no significant difference in $E_{1/2}$ when using the two different methods of analysis. The average error in the DPV $E_{1/2}$ value from independent measurements is ±4 mV (Fig. S2*I*). There is no significant difference in $E_{1/2}$ from α_3Y DP voltammograms obtained by using a GC or a PGE electrode ($\Delta E_{1/2} = 5 \pm 5$ mV). First-derivative analysis was not practical for SWV data due to the increase of noise at higher frequencies. Peak potentials of the net current (E_{net}), forward current (E_{for}), and reverse current (E_{rev}) were obtained by fitting a calculated line to the experimental traces. This is illustrated in Fig. S4 for SW voltammograms obtained over a frequency range of 510 Hz. The average error in E_{net}, E_{for}, and E_{rev} is ±3 mV for data replicates and independent measurements. This is illustrated in Fig. S5.

1. Zheng G, Prince WS (2009) Simultaneous convection compensation and solvent suppression in biomolecular NMR diffusion experiments. *J Biomol NMR* 45:295–299.
2. Bard AJ, Faulkner LR (2001) *Electrochemical Methods: Fundamentals and Applications*, (John Wiley & Sons, Inc., New York), 2nd Ed.
3. Parry EP, Osteryoung RA (1965) Evaluation of analytical pulse polarography. *Anal Chem* 37:1634–1637.
4. Osteryoung J, O'Dea JJ (1986) Square-wave voltammetry. *Electroanalytical Chemistry*, ed Bard AJ (Marcel Dekker, New York), Vol 5, pp 209–308.
5. Mirčeski V, Komorsky-Lovrić Š, Lovrić M (2007) Square-wave voltammetry: Theory and applications. *Monographs in Electrochemistry* ed Scholz F (Springer-Verlag, Berlin).

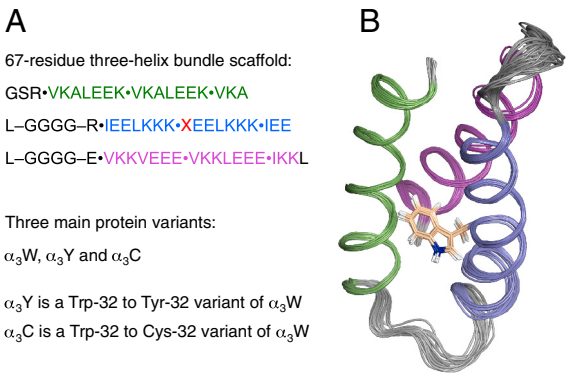

Fig. S1. α_3X family of de novo radical proteins. (*A*) Amino-acid sequence of the three-helix bundle scaffold (helical segments shown in color, loop regions shown in black) that forms the structural platform for a family of de novo proteins constructed to study tyrosine and tryptophan radical chemistry (1). The N-terminal glycine-serine residues form part of a thrombin cleavage site and are numbered as −2 and −1 to keep the amino-acid numbering consistent with the chemically synthesized 65-residue proteins (2). Position 32 (marked with a red X) represents the radical site and contains a tyrosine (in the α_3Y protein), a tryptophan (α_3W), or a cysteine (α_3C). (*B*) Line representation of the 30 refined simulated annealing structures that form the solution NMR structure of α_3W (PDB ID 1LQ7) (3). The side chain of W32 (solvent-accessible surface area 2.6 $\pm$ 1.4% across the NMR structural ensemble) is also shown.

1 Westerlund K, Berry BW, Privett HK, Tommos C (2005) Exploring amino-acid radical chemistry: Protein engineering and de novo design. *Biochim Biophys Acta* 1707:103–116.
2 Tommos C, Skalicky JJ, Pilloud DL, Wand AJ, Dutton PL (1999) *De novo* proteins as models of radical enzymes. *Biochemistry* 38:9495–9507.
3 Dai Q-H, Tommos C, Fuentes EJ, Blomberg MRA, Dutton PL, Wand AJ (2002) Structure of a *de novo* designed protein model of radical enzymes. *J Am Chem Soc* 124:10952–10953.

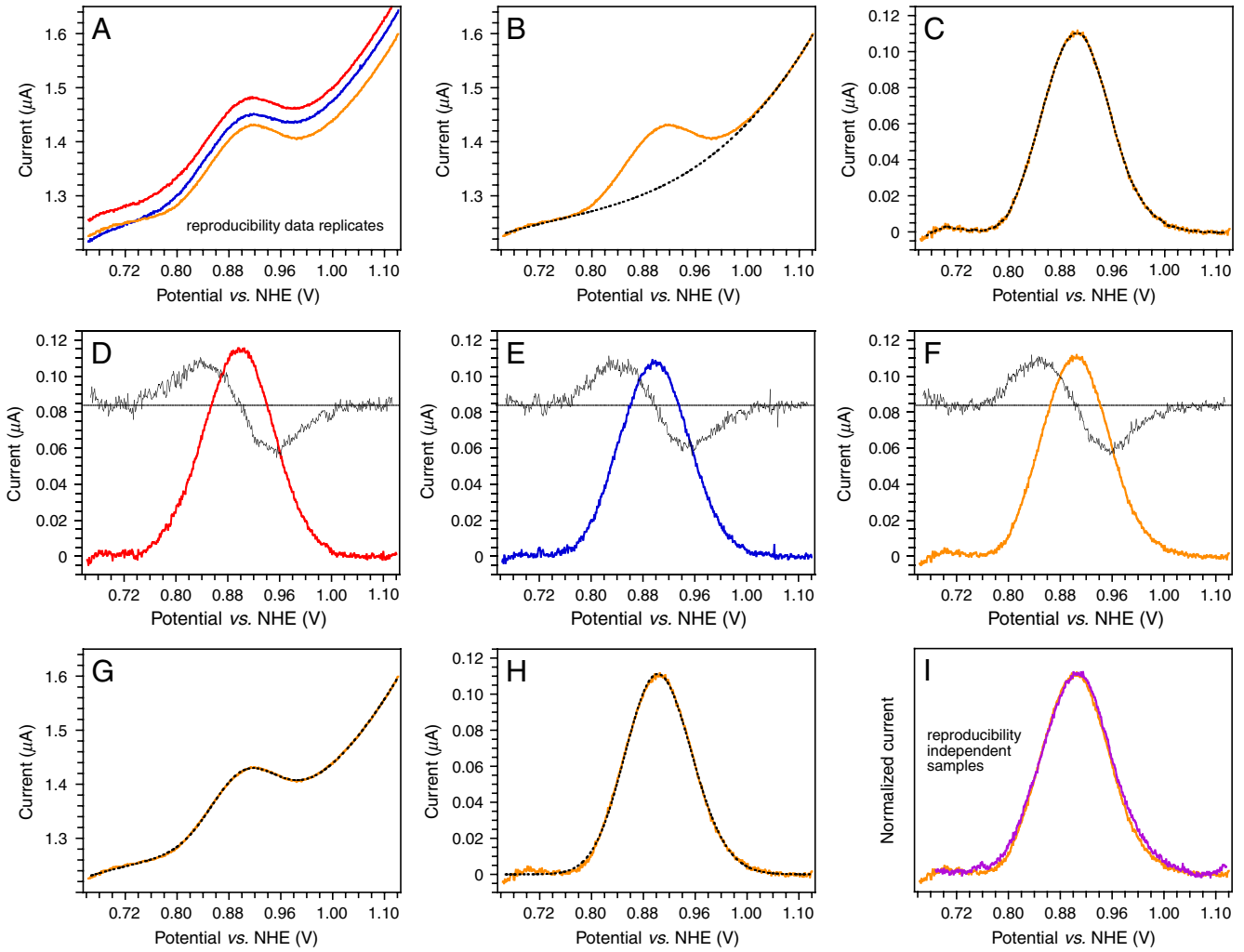

Fig. S2. α_3Y differential pulse voltammograms are highly reproducible. (*A*) α_3Y raw DP voltammograms in triplicate. (*B*) Raw voltammogram (orange) with a fitted cubic baseline (dotted lines). (*C*) Background-corrected (orange) and smoothened (dotted line) trace of the raw voltammogram shown in *B*. Smoothened traces were used in first-derivative analyses to obtain the half-wave potential at maximum current ($E_{1/2}$). (*D–F*) display background-corrected voltammograms (red, blue, and orange) and their first derivatives (black) of the raw voltammograms shown in (*A*). The average $E_{1/2}$ (pH 8.59) value obtained from the zero crossing of the three derivates equal 902 ± 3 mV. (*G*) Raw voltammogram (orange) with a fitted calculated trace (dotted lines). (*H*) Background-corrected traces of the raw and calculated data shown in (*G*). When using this method of analysis, the average $E_{1/2}$ (pH 8.59) equals 899 ± 3 mV for the three raw voltammograms shown in (*A*). (*I*) Background-corrected α_3Y DP voltammograms obtained from two independent measurements using identical experimental settings (pH 8.61 ± 0.02). The average error in the DPV $E_{1/2}$ value derived from independent measurements is ±4 mV. Experimental settings: 200 μM α_3Y in 10 mM sodium acetate, 10 mM potassium phosphate, 10 mM sodium borate, and 100 mM KCl; GC working electrode, temperature 23 °C, interval time 0.1 s, step potential 1.05 mV, scan rate 10.5 mV s^{-1}, modulation time 6 ms, modulation amplitude 50 mV.

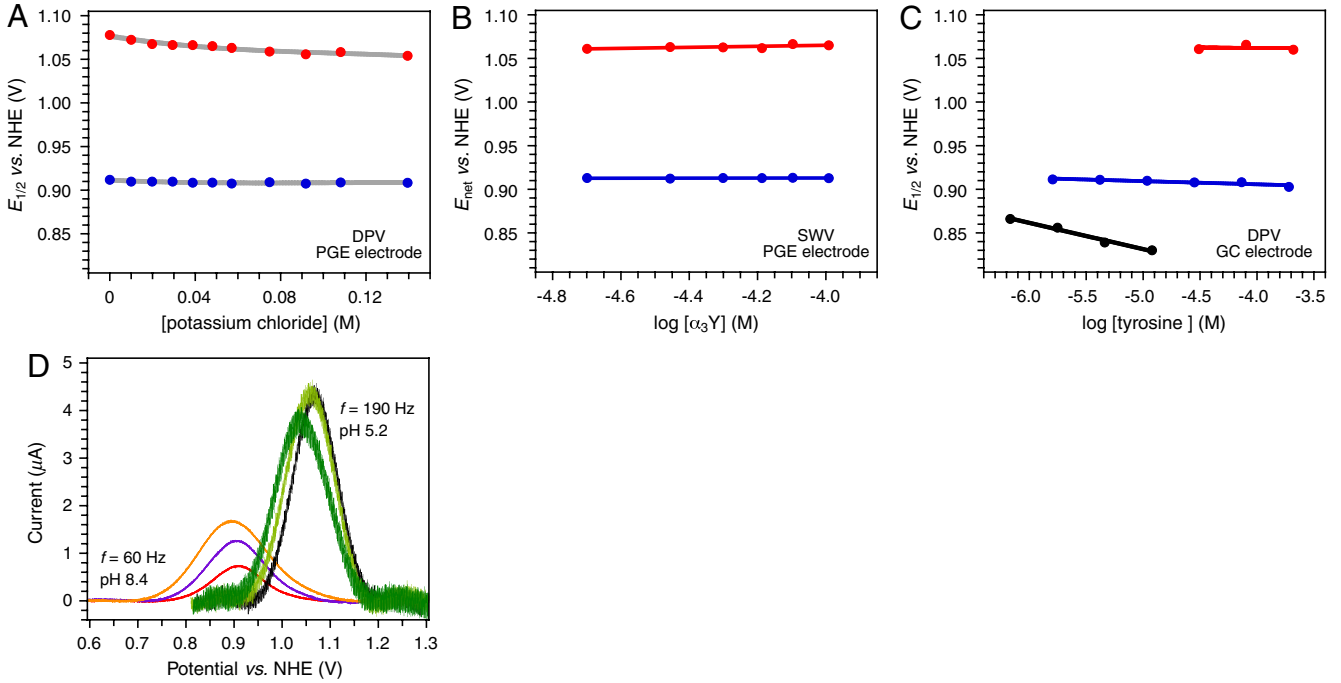

Fig. S3. α_3Y voltammetry optimization and control experiments. DPV can be conducted on α_3Y using either a GC (1) (Fig. S2) or a PGE (*A*) working electrode while SWV can only be performed with a PGE electrode. The Faradaic response observed from α_3Y when using SWV and a GC electrode was overall poor and this approach was not perused beyond a preliminary assessment. (*A*–*D*) represent experiments conducted to optimize sample conditions for SWV and determine the basic PGE electrode characteristics of α_3Y. (*B* and *C*) provide information on the radical mechanism in α_3Y. We start by summarizing the main results concluded from the data shown in (*A*–*D*) and refer to the legends of the individual data boxes for further details. (*i*) Based on the results displayed in (*A* and *B*), we find that 20–100 μM α_3Y in 20 mM sodium acetate, 20 mM potassium phosphate, 20 mM sodium borate, and 80 mM KCl are suitable sample conditions for conducting voltammetry measurements using a PGE electrode. (*ii*) From the data shown in (*B* and *C*) we conclude that peak potentials derived from α_3Y are not influenced by distorting protein/working electrode surface interactions at any conditions used in this study. (*iii*) The data in (*B* and *C*) further confirm that intermolecular radical-radical or radical-protein reactions do not occur for the α_3Y system. This issue is discussed in more detail in the main text. (*iv*) The voltammograms shown (*D*) are consistent with diffusion-controlled electrode kinetics for α_3Y on a PGE electrode at both acidic and alkaline pH. Finally we note that the plots in boxes (*A*–*C*) do contain error bars but they are smaller than the circles representing the data points. (*A*) DPV $E_{1/2}$ potential of α_3Y as a function of the KCl concentration at pH 5.51 ± 0.01 (red circles) and pH 8.40 ± 0.01 (blue circles) using a PGE electrode. The average $E_{1/2}$ (pH 5.51) value decreases by 20 mV as the KCl concentration increases from 0 to 60 mM and then levels out at 1,057 ± 3 mV for the 75–140 mM range. At high pH the $E_{1/2}$ value is independent of the salt concentration with an average $E_{1/2}$ (pH 8.40) value of 909 ± 1 mV across the 10–140 mM range. The S/N of the α_3Y voltammogram declines as the KCl concentration increases and accurate determination of $E_{1/2}$ becomes increasingly more difficult above 140 mM KCl. Based on these results, subsequent PGE-based measurements were carried out with samples containing 20 mM sodium acetate, 20 mM potassium phosphate, 20 mM sodium borate (APB buffer), and 80 mM KCl. Experimental settings: 60 μM α_3Y in 20 mM sodium acetate and 20 mM potassium phosphate (pH 5.51 ± 0.01); 60 μM α_3Y in 20 mM potassium phosphate and 20 mM sodium borate (8.40 ± 0.01); PGE working electrode, temperature 25 °C, interval time 0.1 s, step potential 0.9 mV, scan rate 9.0 mV s^{-1}, modulation time 7–8 ms, modulation amplitude 50 mV. (*B*) SWV E_{net} potential of α_3Y as a function of the protein concentration at pH 5.52 ± 0.01 (red circles) and pH 8.43 ± 0.01 (blue circles) using a PGE electrode. There is no significant change in $\delta E_{net}/\delta \log[\alpha_3 Y]$ at high pH while a minor change in $\delta E_{net}/\delta \log[\alpha_3 Y]$ of 5.9 ± 2.6 mV is observed at low pH. The average E_{net} (pH 5.52; 190 Hz) value is 1,063 ± 2 mV and the average E_{net} (pH 8.43; 190 Hz) value 913 ± 1 mV across a protein concentration range of 20–100 μM. This represents the practical protein concentration range for SWV measurements on α_3Y. The S/N of the Faradaic signal declines at protein concentrations below or above this range. Based on these results, subsequent SWV measurements were carried out with 80 μM α_3Y dissolved in 20 mM APB, 80 mM KCl. Experimental settings: α_3Y in 20 mM APB, 80 mM KCl; PGE working electrode, temperature 25 °C, step potential 0.15 mV, SW pulse amplitude 25 mV, SW frequency 190 Hz. (*C*) DPV $E_{1/2}$ potential of α_3Y as a function of the protein concentration at pH 5.44 ± 0.03 (red circles) and pH 8.66 ± 0.02 (blue circles) using a GC electrode. At low pH there is no significant change in $\delta E_{1/2}/\delta \log[\alpha_3 Y]$ across a protein concentration range of 31–209 μM. The average $E_{1/2}$ (pH 5.44) value is 1,062 ± 5 mV. A small variation in $\delta E_{1/2}/\delta \log[\alpha_3 Y]$ of −3.7 ± 0.9 mV is observed at high pH. The average $E_{1/2}$ (8.66) value is 909 ± 4 mV over a protein concentration range of 2–190 μM. *N*-acetyl-tyrosinamide (NAYA; black circles) dissolved in 20 mM sodium acetate, 20 mM potassium phosphate, 200 mM KCl, pH 5.46 ± 0.01 is shown as an example of a solvated small-molecule system. The variation in $\delta E_{peak}/\delta \log[\text{NAYA}]$ is −30.1 ± 2.6 mV over a concentration range of 680 nM–12 μM. The change in E_{peak} as a function of the NAYA concentration arises from fast intermolecular radical-radical dimerization reactions. This is discussed in more detail in the main text. Experimental settings: α_3Y in 10 mM APB, 100 mM KCl; GC working electrode, temperature 23 °C, interval time 0.1 s, step potential 1.05 mV, scan rate 10.5 mV s^{-1}, modulation time 3–8 ms, modulation amplitude 50 mV. (*D*) Square-wave voltammograms collected from α_3Y as a function of the SW pulse amplitude. These experiments were conduced to investigate whether α_3Y gives rise to adsorption or diffusion-controlled SW voltammograms when using a PGE electrode. (*D*) displays two data sets collected at 190 Hz (pH 5.2 sample) and 60 Hz (pH 8.4 sample). The SW pulse amplitude was 25 mV (red and black traces), 50 mV (blue and light green traces), and 75 mV (orange and medium green traces). For a surface-confined electrode reaction, the net voltammogram may split into two peaks when applying a large overpotential (i.e., pulse amplitudes of 50 and 75 mV) at low SW frequencies (2, 3). The α_3Y voltammogram becomes broader as the pulse amplitude increases, as expected, but the peak maximum remains well defined and there is no indication of a peak splitting. We conclude that the data shown in (*D*) are consistent with diffusion-controlled electrode kinetics at both acidic and alkaline pH. Experimental settings: 80 μM α_3Y in 20 mM APB, 80 mM KCl; PGE working electrode, temperature 25 °C, step potential 0.15 mV, SW pulse amplitude 25, 50, and 75 mV, SW frequency 60 Hz (pH 8.4), and 190 Hz (pH 5.2).

1 Martínez-Rivera MC, Berry BW, Valentine KG, Westerlund K, Hay S, Tommos C (2011) Electrochemical and structural properties of a protein system designed to generate tyrosine Pourbaix diagrams. *J Am Chem Soc* 133:17786–17795.

2 Mirčeski V, Komorsky-Lovrić Š, Lovrić M (2007) Square-wave voltammetry: Theory and applications. *Monographs in Electrochemistry* ed Scholz F (Springer-Verlag, Berlin).

3 Jeuken LJC, McEvoy JP, Armstrong FA (2002) Insights into gated electron-transfer kinetics at the electrode-protein interface: A square wave voltammetry study of the blue copper protein azurin. *J Phys Chem B* 106:2304–2313.

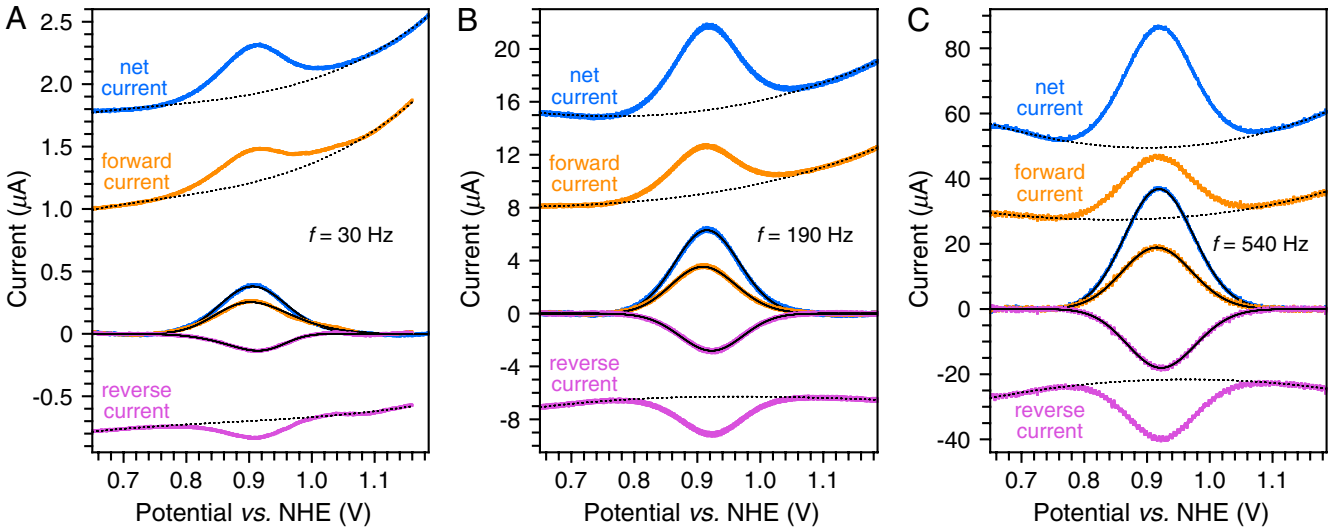

Fig. S4. Typical α_3Y raw and processed square-wave voltammograms. Fig. S4 displays α_3Y voltammograms obtained using a SW frequency of (*A*) 30 Hz (t_p 16.7 ms), (*B*) 190 Hz (t_p 2.6 ms), and (*C*) 540 Hz (t_p 926 μs). (*A* and *B*) display raw traces with the net current in blue, the forward (oxidation) current in orange, and the reverse (reduction) current in purple. The raw traces are shown with the fitted baselines (dotted lines) that were used to generate the background-corrected voltammograms shown in the middle of each data box. The black solid lines represent fitted calculated traces from which peak potentials and peak amplitudes were extracted. The traces obtained at 540 Hz (*C*) were first smoothened using a Savitzky-Golay algorithm (smooth level 0.4%) and then processed as described above for the voltammograms obtained at 30 and 190 Hz. Experimental settings: 80 μM α_3Y in 20 mM APB, 80 mM KCl; PGE working electrode, temperature 25 °C, step potential 0.15 mV, SW pulse amplitude 25 mV.

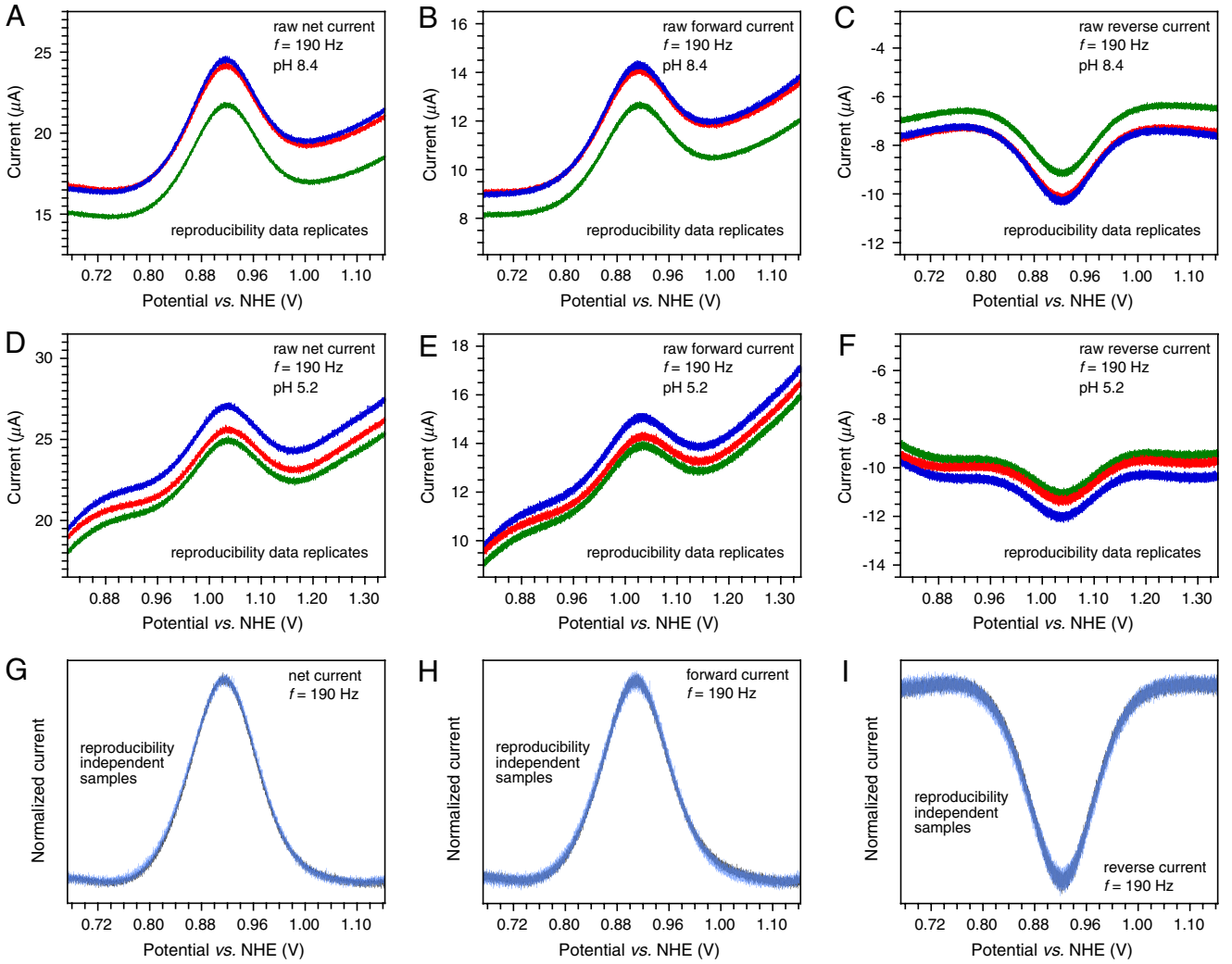

Fig. S5. α_3Y square-wave voltammograms are highly reproducible. Typical α_3Y SW voltammograms with the (*A* and *D*) raw net current and corresponding (*B* and *E*) forward (oxidation) current and (*C* and *F*) reverse (reduction) current displayed in triplicates. The top and middle row represent data collected at alkaline and acidic pH, respectively. The raw traces were processed as described in Fig. S4 with the following results: E_{net} (pH 8.40) 914 ± 1 mV, E_{for} (pH 8.40) 908 ± 1 mV, E_{rev} (pH 8.40) 922 ± 1 mV, and I_{for}/I_{rev} 1.27 ± 0.01. This level of reproducibility was observed for high-pH samples across a 20–100 μM protein range (Fig. S3*B*) and using a SW frequency from 120 (t_p 4.2 ms) to 960 Hz (t_p 521 μs; Fig. 1, main text). The small amplitude of voltammograms obtained at 30 Hz (t_p 16.7 ms; Fig. S4*A*) and 60 Hz (t_p 8.3 ms; Fig. S3*D*) increases the average error bar to ±3 mV (E_{peak}) and ±0.13 (I_{for}/I_{rev}). For the low-pH voltammograms we obtain the following results: E_{net} (pH 5.52) 1,067 ± 2 mV, E_{for} (pH 5.52) 1,062 ± 2 mV, E_{rev} (pH 5.52) 1,074 ± 2 mV, and I_{for}/I_{rev} 1.44 ± 0.03. This level of reproducibility was observed for low-pH samples across a 20–100 μM protein range (Fig. S3*B*) and using a SW frequency of 190 Hz (t_p 16.7 ms) or 540 Hz (t_p 926 μs; Fig. 2, main text). The black and light blue traces displayed in the bottom row represent background-corrected α_3Y (*G*) net, (*H*) forward, and (*I*) reverse SW voltammograms obtained from two independent measurements using identical experimental settings (pH 8.41 ± 0.02). Statistically there is no significant different in the reproducibility observed for data replicates and independent SWV measurements. We conclude that SWV studies on α_3Y yield highly reproducible results with an average error bar of ±3 mV in E_{peak}. Experimental settings: 80 μM α_3Y in 20 mM APB, 80 mM KCl; PGE working electrode, temperature 25 °C, step potential 0.15 mV, SW pulse amplitude 25 mV, SW frequency 190 Hz.

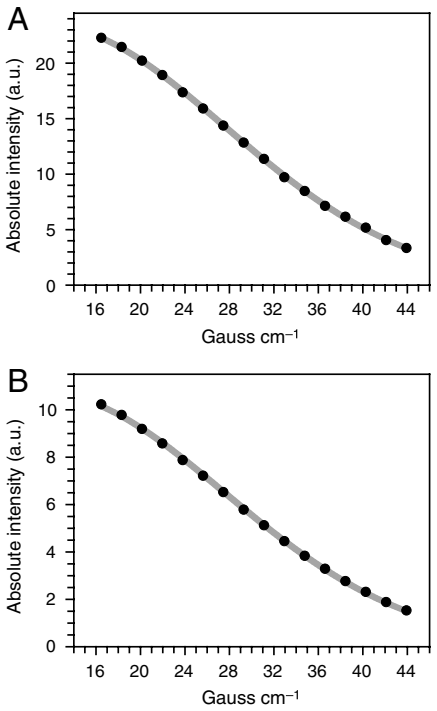

Fig. S6. Determination of the α_3Y diffusion coefficient by pulsed field gradient NMR. Diffusion attenuation plots of α_3Y (*A*) amide protons and (*B*) aliphatic protons. The plots are fitted to Eq. **9** in ref. 1 and provided a diffusion coefficient for α_3Y of $1.47 \pm 0.01 \times 10^{-6}$ $cm^2\,s^{-1}$. Experimental settings: 500 μM α_3Y in 20 mM deuterated sodium acetate, 20 mM potassium phosphate, 20 mM sodium borate, 140 mM KCl, 5% D_2O, pH 6.6; temperature 25 °C.

1 Zheng G, Prince WS (2009) Simultaneous convection compensation and solvent suppression in biomolecular NMR diffusion experiments. *J Biomol NMR* 45:295–299.